A pilot study of changes in ^{18}F-FDG uptake, calcification and global metabolic activity of the aorta with aging

Gonca G. Bural,
Drew A. Torigian,
Elias Botvinick,
Mohamed Houseni,
Sandip Basu,
Wengen Chen,
Abass Alavi

Division of Nuclear Medicine, Department of Radiology, University of Pennsylvania School of Medicine.

Keywords:
– ^{18}F-FDG-PET
– Contrast enhanced computed tomography
– Atherosclerosis
– Aorta calcification
– Global metabolic activity

Correspondence address:
Drew A. Torigian, MD, MA
Department of Radiology
Hospital of the University of Pennsylvania 3400 Spruce Street, Philadelphia, PA 19104, USA
Phone: 215-615-3805
Fax: 215-614-0033
Email: Drew.Torigian@uphs.upenn.edu

Received:
30 March 2009
Accepted revised:
24 April 2009

Abstract

Our aim was to quantify changes in the inflammatory and calcific components of atherosclerosis in the aortic wall using fluoro-18-2-fluoro-2-deoxy-D-glucose positron emission tomography ^{18}F-FDG-PET and contrast enhanced computerized tomography (CECT) with increasing age. *Twelve subjects*, 8 men and 4 women aged from 21-80 years who had both ^{18}F-FDG-PET and CECT of the chest and abdomen were included in this study. Subjects were grouped into three according to age. ^{18}F-FDG uptake in four segments of the aorta was measured. Using CECT images, aortic segmental wall volumes were measured. Wall calcification volume in each aortic segment was also measured via adaptation of a coronary artery calcium-scoring program to the aorta. Calcification volumes were then subtracted from aortic wall volumes. Each net segmental aortic wall volume was then multiplied by the accompanying mean SUV of the segment to calculate global metabolic activity (GMA) for each aortic segment. *Our results showed* that in each aortic wall segment, mean SUV, wall volumes, wall calcification volumes, and GMA statistically significantly increased with age. *In conclusion*, ^{18}F-FDG uptake, wall volume, wall calcification volume, and GMA in the aorta increase with aging. The ^{18}F-FDG uptake represents the early inflammatory component of the atherosclerotic process, whereas calcification generally represents a later and irreversible stage of the disease. Measurement and combination of PET and CECT parameters to calculate GMA may allow for optimal morphologic and functional noninvasive quantitative assessment of global aortic atherosclerotic disease.

Hell J Nucl Med 2009; 12(2): 123-128 • Published on line: 28 May 2009

Introduction

In the United States and other Western countries, atherosclerosis is the leading cause of illness and death [1, 2]. By 2020, it is predicted to be the number one cause of death worldwide [3]. It is a slow progressive process that may start in childhood [4-7]. Atherosclerosis is a systemic chronic, inflammatory disease characterized by over-recruitment of leukocytes (monocytes and T-cells) to sites of inflammation [8, 9]. From the initial phases of disease, through to its phase of slow progression, and finally to the phase of clinical complications, inflammation has fundamental importance in all phases of atherosclerosis [10]. Atherosclerosis begins when monocytes migrate from the bloodstream into the wall of the artery and become macrophages that accumulate fatty materials. In time, these fat-laden macrophages accumulate, leading to a patchy thickening in the inner lining of the artery. Each area of thickening (the atherosclerotic plaque or atheroma) is filled with a combination of triglycerides, cholesterol, inflammatory cells and connective tissue cells [11]. Plaques generally continue to change and progressively enlarge through cell death and degeneration. Calcification, which is a late and generally irreversible component of the atherosclerotic process, tends to be observed in advanced atherosclerosis.

The ideal clinical modality for imaging and quantifying atherosclerosis should be safe, noninvasive, accurate, and reproducible, thus allowing for longitudinal studies in patients. Fluorine-18-2-fluoro-2-deoxy-D-glucose positron emission tomography (^{18}F-FDG-PET) is an ideal imaging modality to non-invasively quantify the early inflammatory component of atherosclerosis. It is possible to image whole segments of the aorta with a whole body ^{18}F-FDG-PET scan. The uptake of ^{18}F-FDG is a measure of metabolic activity of atherosclerotic lesions [12]. The severity of the inflammatory process in the arterial wall can be semi-quantitatively measured by using standardized uptake values (SUV).

As a functional imaging modality, ^{18}F-FDG-PET alone may have limitations in quantifying the extent and composition of atherosclerosis particularly in advanced stages, since it does not give any morphological information about the arterial wall such as thickness, volume, or presence and volume of calcification. However, contrast enhanced computed tomography (CECT), an anatomical imaging modality, can be used to assess arterial wall thick-

ness and volume, as well as calcification volume. Use of the combination of the quantitative functional and anatomical data obtained from these imaging modalities is therefore the logical approach to assess the atherosclerotic activity -global metabolic activity (GMA) of an artery.

Our objectives in conducting this research were to quantify changes in aortic wall ^{18}F-FDG uptake, aortic wall volume, aortic wall calcification volume, and aortic GMA with increasing age through use of ^{18}F-FDG-PET and CECT.

Subjects and methods

This study was approved by our institutional review board as a retrospective study prior to study initiation.

Study population

Subjects were retrospectively selected amongst those who had both whole body ^{18}F-FDG-PET scans and routine contrast enhanced CECT scans of the chest and abdomen within a six month interval. PET and CECT studies were performed within a time interval of 0-180 days. These subjects were then divided into three groups according to their age 21-40 years, 41-60 years, and 61-80 years. Two of the five subjects in the first group had diagnosis of cervical cancer, two had Hodgkin's disease, and one had pulmonary thromboembolism. In the second group, one of four subjects had multiple myeloma, one had esophageal cancer, one renal cell carcinoma, and one had colon cancer. In the last group of 3 subjects, 2 had lung cancer and 1 had a benign solitary pulmonary nodule. None of these patients had evidence for cardiovascular disease as based on clinical record review and electrocardiogram findings.

^{18}F-FDG-PET imaging and analysis

PET imaging was performed on a dedicated whole body PET scanner (Allegro; Philips Medical Systems, Bothell WA, USA). At the time of ^{18}F-FDG injection all subjects had fasted for at least 4h and had blood sugar levels of <150mg/dL. Image acquisition for the whole body scan started at a mean time point of 60min after injection of 2.52MBq/kg of body weight. Scanning included the neck, thorax, abdomen, pelvis, and upper thighs. Images consisted of 4 or 5 emission frames of 25.6cm length with an overlap of 12.8cm covering an axial length of 64-76.8cm. Image reconstruction was performed with an iterative ordered-subsets expectation maximization algorithm with 4 iterations and 8 subsets. Attenuation-corrected images were obtained by applying transmission maps with a cesium-137 source interleaved with the emissions scans.

The degree of ^{18}F-FDG uptake in 4 wall segments of the aorta (ascending, arch, descending thoracic, and abdominal) was measured by recording the mean SUV in each segment for each subject (Fig. 1). The mean SUV of each segment was determined by placing 4 to 6 regions of interest (ROI) in each transverse section (Fig. 2). After calculating the mean values for each particular section, mean SUV for all transverse sections for each segment were summed, and the arithmetical mean of these values for that segment was calculated. No attempt was made to correct for partial volume effects.

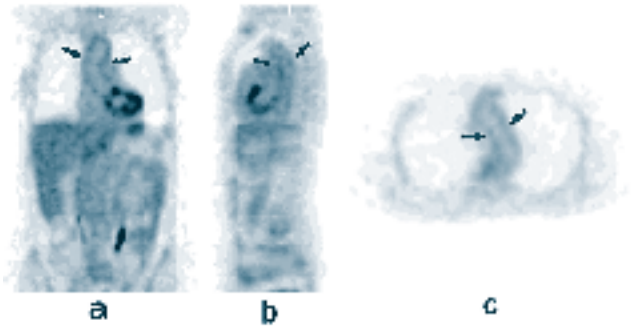

Figure 1. Coronal (a), sagittal (b), and transverse (c) slices of ^{18}F-FDG-PET images. There is visible ^{18}F-FDG uptake in walls of ascending, arch, and descending aorta (arrows) in this 32 years old subject. Mean SUV for ascending, arch, and descending aorta was 1.5.

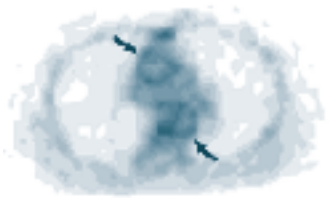

Figure 2. Transverse slice of ^{18}F-FDG-PET image. Note ^{18}F-FDG uptake in ascending and descending aorta (arrows).

CECT imaging and analysis

Pre- and post- CECT angiographic examinations of the chest and abdomen performed within 6 months of ^{18}F-FDG-PET scans for this subject sample were independently analyzed on a dedicated 3D workstation (Advantage Workstation 4.0; GE Medical Systems, Milwaukee, Wisconsin, USA). On each CECT image, inner and outer surfaces of the aortic wall were visually identified, and manual tracings along the contours of these surfaces were created with a mouse and an electronic curve-drawing tool (Fig. 3). Quantitative values of the areas contained within the inner and outer tracings were automatically generated by the software and recorded. Tracings were performed from the aortic root through the ascending aorta, aortic arch, descending thoracic aorta to the level of the celiac artery, and

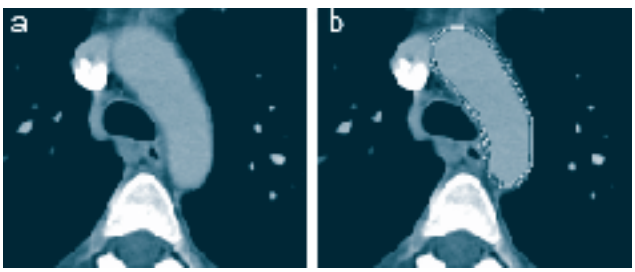

Figure 3. Aortic wall volume measurement, methodology. a, On transverse thoracic contrast enhanced CECT image arch of aorta is visible. b, On the same CECT image aortic arch walls are delineated with manually drawn ROI. Inner ROI was drawn around aortic lumen. Outer ROI was placed on outer aortic contour. Cross-sectional area values were then calculated by subtracting inner area from the outer area. This procedure was repeated for all transverse slices through entire aorta.

abdominal aorta. Inner and outer tracing area values were then summed separately for each of the 4 arterial segments, and the total inner area sum for each segment was then subtracted from the total outer area sum for each segment. These area values for each arterial segment were then multiplied by the nominal slice thickness of the CECT examination to lead to values of arterial wall volume for each aortic segment.

The amount of aortic wall calcification was then calculated in each aortic segment by adaptation of a validated coronary artery calcium scoring program (Syngo Calcium Scoring; Siemens Medical Systems, Malvern, Pennsylvania, USA) (Fig. 4) to the aorta. This analysis was performed using the unenhanced CECT images that were part of the CECT angiographic studies. Subsequently, aortic segmental calcification volumes were subtracted from associated aortic segmental wall volumes to calculate net segmental (non-calcified) aortic wall volumes corresponding to the likely site of ^{18}F-FDG uptake.

Calculation of global metabolic activity of the aorta

After subtracting aortic wall calcification volume from aortic wall volume to obtain net aortic wall volume, we multiplied this by the mean SUV to obtain GMA with units of cm^3-SUV for each aortic segment, and subsequently summed these over the 4 aortic segments to obtain the GMA for the entire aorta. Two different sets of anatomic and metabolic data were combined into a new single quantitative parameter, GMA, which summarizes information about the total atherosclerotic burden of the aorta.

Assessment of aortic wall, ^{18}F-FDG uptake, volume, calcification volume, and GMA with aging

Means and standard deviations for aortic SUV, wall volumes, wall calcification volumes, and GMA values were subsequently calculated for each of the three age groups. All data acquired from quantitative analysis were recorded into a computerized spreadsheet (Microsoft Excel 2002; Microsoft Corporation, Redmond, Washington, USA). These data were then compared amongst the three different age groups. Statistical analysis was performed using statistical software (InStat 2003; GraphPad Software Inc., San Diego, California, USA). An analysis of variance appropriate for a non-repeated one-factor design was used to assess for significant differences between aortic mean SUV, wall volumes, wall calcification volumes, and GMA values amongst the different age groups using a P value of <0.05 as the threshold for statistical significance. Newman-Keuls multiple comparison testing was then used for the aortic segments and the entire aorta to assess for significant differences in the parameters listed above between the three age groups. The correlation between mean aortic wall ^{18}F-FDG SUV and age, total aortic wall calcification volume with age, and GMA with age were assessed by using Pearson correlation testing.

Results

Mean SUV of each aortic segment and for the entire aorta for different age groups are given in Table 1. Mean SUV increased for the aortic segments and for the entire aorta as the age of the group increased. There was a statistically significant difference for mean SUVs amongst the first and third age groups for all aortic segments. Newman-Keuls multiple comparison testing demonstrated statistically significant differences in mean SUVs between all age groups for the ascending aorta, between the 21-40 and 41-60 as well as between the 21-40 and 61-80 age groups for the arch of the aorta, between the 21-40 and 61-80 age groups for the abdominal aorta, and between the 21- 40 and 41-60 and between the 21-40 and 61-80 age groups for the entire aorta.

Figure 4. Transverse thoracic unenhanced CECT image, with very high attenuation- calcification in the wall of arch of aorta (arrows). Calcification in walls of aortic segments was detected via adaptation of coronary calcium scoring software.

Aortic wall volumes assessed from CECT images for different age groups are given in Table 2. Mean aortic wall volumes increased for the groups as age increased. There were statistically significant differences for mean aortic wall volumes amongst the three age groups for all aortic segments. Newman-Keuls multiple comparison testing demonstrated statistically significant differences for aortic wall volumes between the 21-40 and 61-80 age groups as well as the 41-60 and 61-80 age groups for the ascending aorta, between the 21-40 and 41-80 age groups and between the 21-60 and 61-80 age

Table 1. *Mean SUV (and SD) for each aortic segment and the entire aorta*

Age	Ascending aorta	Arch of aorta	Descending thoracic aorta	Abdominal aorta	Aorta
21-40 (n = 5)	1.5±0.2	1.5±0.3	1.7±0.3	1.6±0.1	1.5±0.2
41-60 (n =4)	1.9±0.1	1.9±0.2	2.1±0.5	1.9±0.2	1.9±0.2
61-80 (n = 3)	2.2±0.1	2.1±0.1	2.4 ± 0.3	2.0±0.1	2.2±0.1
P values	0.001	0.02	0.04	0.01	0.001

Table 2. *Wall volumes in cm^3 (mean and SD) for each aortic segment and the entire aorta*

Age	Ascending aorta	Arch of aorta	Descending thoracic aorta	Abdominal aorta	Aorta
21-40 (n = 5)	2.5±0.8	3.9±1.0	6.6±1.4	3.3±1.3	17.1±4.3
41-60 (n =4)	3.9±1.5	6.1±1.3	9.2±4.1	8.9±3.3	28.2±3.1
61-80 (n = 3)	7.1±0.2	7.6±1.5	16.5±7.3	14.4±5.9	45.7±11.7
P values	0.0005	0.01	0.03	0.001	0.001

groups for the arch of the aorta, and between the 21-40 and 61-80 age groups for descending thoracic and abdominal aorta. There was a statistically significant difference in entire aortic wall volume between all age groups.

In Table 3, mean aortic wall calcification volumes and standard deviations for each aortic segment and for the entire aorta are given. In the youngest group, no subject revealed calcification in the aorta. In the middle aged group, the ascending aorta and arch of the aorta did not reveal calcification, but descending and abdominal aortic segments did reveal calcification. In the oldest age group, all segments revealed calcification. There were statistically significant differences for wall calcification volumes amongst three age groups for all aortic segments. Newman-Keuls multiple comparison testing demonstrated statistically significant differences between the 21-40 and 61-80 age groups and between the 41-60 and 61-80 age groups for the arch of the aorta, the descending thoracic aorta, and for the entire aorta.

GMA of the aortic segments (calculated by multiplication of the mean SUV of each aortic segment by net segmental aortic wall volume, i.e. wall volume minus wall calcification volume) with units of cm^3-SUV are given in Table 4. Newman-Keuls multiple comparison testing demonstrated statistically significant differences for GMA between the 21-40 and 61-80 age groups and between the 41-60 and 61-80 age groups for the ascending aorta, and between the 21-40 and 61-80 age groups for the descending thoracic aorta.

The mean aortic wall ^{18}F-FDG uptake, calculated by averaging the mean SUV in all four aortic segments, showed a positive correlation with age (r=0.89, P<0.05). Figure 5 shows the relationship of ^{18}F-FDG uptake in the aortic wall with aging. The total wall calcification volume in the entire aorta also showed a positive correlation with age (r=0.67, P<0.05). The total aortic wall calcification volume for each subject is shown to vary with age in Figure 6. GMA of the entire aorta showed a positive correlation with age (r= 0.67, P<0.05), and is shown in Figure 7.

Table 3. *Calcification volumes in cm^3 (mean and SD) for each aortic segment and the entire aorta*

Age	Ascending aorta	Arch of aorta	Descending thoracic aorta	Abdominal aorta	Aorta
21-40 (n = 5)	0	0	0	0	0
41-60 (n =4)	0	0	0.23±0.30	0.19±0.28	0.42±0.23
61-80 (n = 3)	0.14±0.17	0.21±0.14	0.72±0.47	3.65±3.86	5.43±4.50
P values	0.07	0.01	0.02	0.03	0.01

Table 4. *Global metabolic activity in cm^3 - SUV (mean and SD) for each aortic segment and entire aorta*

Age	Ascending aorta	Arch of aorta	Descending thoracic aorta	Abdominal aorta	Aorta
21-40 (n = 5)	4.0±1.6	6.0±1.6	10.5±3.5	9.6±4.0	30.2±10.5
41-60 (n =4)	7.5±2.8	11.7±2.4	17.7±9.3	22.6±5.9	59.6±10.5
61-80 (n = 3)	15.8±4.2	11.8±6.2	31.8±15.2	26.8±15	76.1±51.4
P values	0.0001	0.05	0.03	0.03	0.05

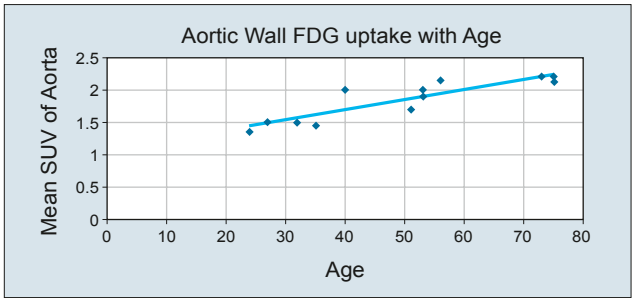

Figure 5. Change in aortic wall ^{18}F-FDG uptake with age. Note linear increase of mean SUV in aorta with increasing age.

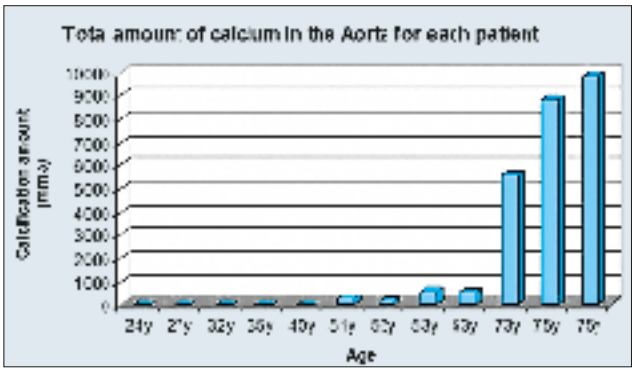

Figure 6. Total wall calcification volume in entire aorta for individual subjects of varying age. Note presence of aortic calcification in subjects greater than 50 years old, and highest calcification volumes in subjects from oldest age group

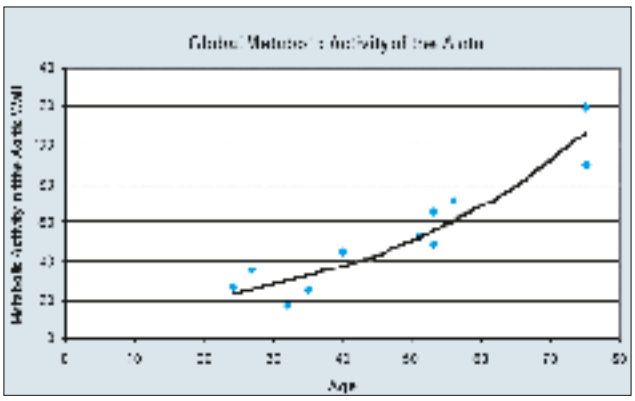

Figure 7. Change in GMA of aorta with age. Note exponential increase of aortic GMA with increasing age.

Discussion

Atherosclerosis is a chronic progressive disease that generally has a long asymptomatic phase. It begins early in life as an asymptomatic disease process, and is associated with cardiovascular risk factors [13]. After initial disruption of the intimal

layer, macrophages start to accumulate fatty materials. In time, accumulation of these fat-laden macrophages leads to a thickening of the intimal layer, which then develops into mature atherosclerotic plaque. As the plaque increases over time, the vessel may expand, so that luminal diameter and therefore blood flow are preserved, known as positive remodeling [14].

Usually, atherosclerosis does not produce clinical symptoms until it leads to arterial narrowing or obstruction. Angiography may not detect atherosclerotic lesions that do not lead to luminal narrowing and provides minimal information about atherosclerotic plaque composition. Therefore, it is no longer been considered the gold standard imaging technique for detection or quantitation of atherosclerosis [14]. Several other noninvasive imaging modalities have been used to assess atherosclerosis. Magnetic resonance imaging, ultrasonography and CECT are recognized imaging modalities that have been used to evaluate atherosclerotic plaque composition and disease burden in different arteries [15-20]. These imaging modalities focus on structural alterations in the arterial wall and do not take into account the metabolic alterations that may also be present in earlier stages of disease.

Other diagnostic modalities are therefore needed to evaluate the full degree and the extent of atherosclerosis. The inflammatory process plays a key role in all phases of atherosclerosis. Therefore, ^{18}F-FDG-PET is a novel approach for quantitative measurement of disease activity in atherosclerosis [12]. Studies from laboratory data have shown that in the arterial wall, ^{18}F-FDG is taken up by inflammatory cells, predominantly macrophages, in atherosclerotic plaque [21, 22]. This accumulation was initially reported to be due to atherosclerosis [23], and then reported as a manifestation of the inflammatory component of atherosclerosis [24-27].

Calculation of the mean SUV on ^{18}F-FDG-PET images of an aortic segment provides quantitative information about the severity of the inflammatory process in each aortic segment. In the present study, we calculated the mean SUV for each of four aortic segments, which can easily be assessed on ^{18}F-FDG-PET images. In each segment, continuous radiotracer uptake was noted in the aortic wall, which made it possible to put several ROI over the aortic wall to calculate mean SUV. Calculation of mean SUV separately for each arterial segment is important to provide regional information to assess the degree of the inflammatory process in different aortic segments.

The non-calcified aortic wall is the potential space for the accumulation of ^{18}F-FDG. In our analysis, we have assumed that the calcified areas within the aortic wall are no longer metabolically active, and therefore, no longer have ^{18}F-FDG uptake. Therefore the potential volume for ^{18}F-FDG accumulation within the aortic wall can be calculated by subtracting total aortic wall calcification volume from total aortic wall volume.

After subtracting aortic wall calcification volume from aortic wall volume to obtain net aortic wall volume, we multiplied this by the mean SUV to obtain GMA for each aortic segment, and subsequently summed these over the 4 aortic segments to obtain the GMA for the entire aorta. This approach combines two different sets of anatomic and metabolic data into a new single quantitative parameter, GMA, which summarizes information about the total atherosclerotic burden of the aorta.

In the present study, we observed an increase in ^{18}F-FDG uptake in the wall of all aortic segments with increasing age, and the correlation between total aortic ^{18}F-FDG uptake and age was high (r=0.88). This likely reflects a cumulative increase in the severity of the ongoing inflammatory process within the aortic wall with increasing age. Interestingly, we noted that ^{18}F-FDG uptake in the aortic wall is commonly seen in relatively young individuals, although this is not an unexpected observation as atherosclerosis often begins early in life [5] and ^{18}F-FDG-PET is exquisitely sensitive to the presence of early disease [28].

Atherosclerotic plaque usually undergoes calcification in later stages of the disease. A positive correlation has been reported in the literature between abdominal aortic calcification and older age [29]. Our findings are in agreement with this report. In our study, we found a positive correlation between total aortic wall calcification and increasing age. There was no visible aortic wall calcification on CECT images in the first group of subjects between the ages of 21 and 40 years, but the degree of visible calcification appeared to be most extensive in the oldest age group between the ages of 61 and 75 years.

CECT can also detect the anatomic effects of plaque accumulation and arterial wall remodeling. Arterial wall volume, which we have measured from CECT images, is an indicator of atherosclerotic positive remodeling [29]. In this study, we showed that aortic wall volume also increases with increasing age. Macroscopic structural changes of atherosclerosis involving the aorta assessed with CECT, such as increasing wall volume and wall calcification volume, generally occur in the later stages of the atherosclerotic process, whereas cellular and molecular changes in the aortic wall as seen on ^{18}F-FDG-PET imaging are generally detected earlier in the disease process.

In our study, we found that GMA increased regionally in each aortic segment and in the entire aorta as age increased. GMA values also showed a positive correlation with increasing age. These findings are a manifestation of an increase in plaque accumulation and aortic wall remodeling over time, in keeping with age as a non-modifiable risk factor for atherosclerosis. As atherosclerosis is a systemic disease of the arterial tree, GMA of the aorta may therefore serve as an indirect indicator of the overall atherosclerotic process affecting the entire arterial tree. Several studies support this hypothesis [30-34]. As there is a need for a noninvasive means of detecting subclinical arterial disease [35], GMA quantification via ^{18}F-FDG-PET and CECT imaging may potentially be useful as a screening test to predict for future clinically significant events, although further prospective research studies will be required to make this determination. GMA can also potentially be used to noninvasively assess the effects of treatment targeted against atherosclerosis such as with lipid lowering agents.

Our study has several limitations. One limitation was the small sample size. This was in part related to exclusion of sev-

eral subjects from the oldest age group, as the calcium-scoring program was not able to completely segment the wall calcification in the abdominal aorta, particularly when an abdominal aneurysm was located adjacent to the lumbar spine, which has very high attenuation related to calcium content similar to calcification occurring in the aortic wall. Another limitation of this study was its retrospective nature, which prevented us from accumulating all pertinent data with regards to cardiovascular risk factors. Furthermore, no attempt was made to correct for partial volume effects upon SUV measurements related to aortic wall thickness, although such effects can be addressed in future studies. Lastly, ^{18}F-FDG-PET and CECT studies were performed with an intervening time interval of up to 180 days, although the same day imaging would have been ideal, and can also be performed in future prospective studies through use of PET/CECT technology.

In conclusion, the early inflammatory component of aortic atherosclerosis can be detected using ^{18}F-FDG-PET imaging, and tends to increase with age. Aortic wall calcification due to atherosclerosis is also grossly detectable on CECT and also increases in volume with age, although it is detected at a later age than the inflammatory component of atherosclerosis. Assessment of aortic GMA combines data regarding metabolic and anatomical changes of the atherosclerotic process into a single quantitative parameter. As such, aortic GMA may be a useful parameter to noninvasively assess a patient's risk for future clinical events related to atherosclerosis, and to monitor the effects of treatment directed toward atherosclerosis.

Bibliography

1. Breslow JL. Cardiovascular disease burden increases, NIH funding decreases. *Nat Med* 1997; 3: 600-601.
2. Braunwald E. Shattuck lecture. Cardiovascular medicine at the turn of the millennium: triumphs, concerns, and opportunities. *N Engl J Med* 1997; 337: 1360-1369.
3. Scott J. The pathogenesis of atherosclerosis and new opportunities for its treatment and prevention *J Neural Transm* 2002; 63(Suppl): 1-17.
4. Kortelainen ML. Adiposity, cardiac size and precursors of coronary atherosclerosis in 5 to 15-year-old children: a retrospective study of 210 violent deaths. *Int J Obes Relat Metab Disord* 1997; 21: 691-607.
5. Daniels SR. Cardiovascular disease risk factors and atherosclerosis in children and adolescents. *Curr Atheroscler Rep* 2001; 3: 479-485.
6. Berenson GS, Srinivasan SR, Bao W et al. Association between multiple cardiovascular risk factors and atherosclerosis in children and young adults: the Bogalusa Heart Study. *N Engl J Med* 1998; 338: 1650-1656.
7. Jarvisalo MJ, Jartti L, Nanto-Salonen K et al. Increased aortic intima-media thickness: a marker of preclinical atherosclerosis in high-risk children. *Circulation* 2001; 104: 2943-2947.
8. Steffens S, Mach F. Inflammation and Atherosclerosis. *Herz* 2004; 29: 741-748.
9. Hawkins MA. Markers of increased cardiovascular risk: are we measuring the most appropriate parameters? *Obes Res* 2004; 12: 107-14S.
10. Libby P. Vascular biology of atherosclerosis: overview and state of the art. *Am J Cardiol* 2003; 91: 3A-6A.
11. Hanke H, Lenz C, Finking G. The discovery of the pathophysiological aspects of atherosclerosis. A review. *Acta Chir Belg* 2001; 101: 162-169.
12. Weissberg PL. Noninvasive imaging of atherosclerosis: the biology behind the pictures. *J Nucl Med* 2004; 45: 1794-1795.
13. Duprez DA, Cohn JN. Monitoring vascular health beyond blood pressure. *Curr Hypertens Rep* 2006; 8: 287-291.
14. Davies JR, Rudd JH, Weissberg PL. Molecular and metabolic imaging of atherosclerosis. *J Nucl Med* 2004; 45: 1898-1907.
15. Rutt BK, Clarke SE, Fayad ZA. Atherosclerotic plaque characterization by MR imaging. *Curr Drug Targets Cardiovasc Haematol Disord* 2004; 4: 147-159.
16. Mancini GB, Abbott D, Kamimura C, Yeoh E. Validation of a new ultrasound method for the measurement of carotid artery intima medial thickness and plaque dimensions. *Can J Cardiol* 2004; 20: 1355-1359.
17. Schoepf UJ, Becker CR, Ohnesorge BM, Yucel EK. CT of coronary artery disease. *Radiology* 2004; 232: 18-37.
18. Takasu J, Mao S, Budoff MJ. Aortic atherosclerosis detected with electron-beam CT as a predictor of obstructive coronary artery disease. *Acad Radiol* 2003; 10: 631-637.
19. Inoue F, Sato Y, Matsumoto N et al. Evaluation of plaque texture by means of multislice computed tomography in patients with acute coronary syndrome and stable angina. *Circ J* 2004; 68: 840-844.
20. Becker CR, Nikolaou K, Muders M. Ex vivo coronary atherosclerotic plaque characterization with multi-detector-row CT. *Eur Radiol* 2003; 13: 2094-2098.
21. Rudd JH, Warburton EA, Fryer TD et al. Imaging atherosclerotic plaque inflammation with ^{18}F-fluorodeoxyglucose positron emission tomography. *Circulation* 2002; 105: 2708–2711.
22. Ogawa M, Ishino S, Mukai T et al. ^{18}F-FDG accumulation in atherosclerotic plaques: immunohistochemical and PET imaging study. *J Nucl Med* 2004; 45: 1245-1250.
23. Yun M, Yeh D, Araujo LI et al. ^{18}F-FDG uptake in the large arteries: a new observation. *Clin Nucl Med* 2001; 26: 314-319.
24. Ben-Haim S, Kupzov E, Tamir A, Israel O. Evaluation of ^{18}F-FDG uptake and arterial wall calcifications using 18F-18F-FDG PET/CT. *J Nucl Med* 2004; 45: 1816-1821.
25. El-Haddad G, Zhuang H, Gupta N, Alavi A. Evolving role of positron emission tomography in the management of patients with inflammatory and other benign disorders. *Semin Nucl Med* 2004; 34: 313-329.
26. Zhuang H, Alavi A. ^{18}F-FDG-PET Imaging in the Detection and Monitoring Infections and Inflammation. *Semin Nucl Med* 2002; 32: 47-59.
27. Jayalath RW, Mangan SH, Golledge J. Aortic calcification. *Eur J Vasc Endovasc Surg* 2005; 30: 476-488.
28. Bural GG, Torigian DA, Chamroonrat W et al. FDG-PET is an effective imaging modality to detect and quantify age-related atherosclerosis in large arteries. *Eur J Nucl Med Mol Imaging* 2008;35:562-569.
29. Crouse JR 3rd. Imaging atherosclerosis: State of the art. *J Lipid Res* 2006; 47: 1677-1699.
30. Bocchio M, Scarpelli P, Necozione S et al. Intima-media thickening of common carotid arteries is a risk factor for severe erectile dysfunction in men with vascular risk factors but no clinical evidence of atherosclerosis. *J Urol* 2005; 173: 526-529.
31. Poredos P. Intima-media thickness: indicator of cardiovascular risk and measure of the extent of atherosclerosis. *Vasc Med* 2004; 9: 46-54.
32. de Groot E, Hovingh GK, Wiegman A et al. Measurement of arterial wall thickness as a surrogate marker for atherosclerosis. *Circulation* 2004; 109 Suppl: III33-III338.
33. Prasad Y, Bhalodkar NC. Aortic sclerosis; a marker of coronary atherosclerosis. *Clin Cardiol* 2004;27:671-673.
34. Markopoulos C, Mantas D, Revenas K et al. Breast arterial calcifications as an indicator of systemic vascular disease. *Acta Radiol* 2004; 45: 726-729.
35. Simon A, Chironi G, Levenson J. Performance of subclinical arterial disease detection as a screening test for coronary heart disease. *Hypertension* 2006; 48: 392-396.